Journal of Controlled Release 196 (2014) 332–343

Contents lists available at ScienceDirect

Journal of Controlled Release

journal homepage: www.elsevier.com/locate/jconrel

Monoclonal antibody-targeted, temperature-sensitive liposomes: In vivo tumor chemotherapeutics in combination with mild hyperthermia

Zahraa S. Al-Ahmady [a,b], Olivier Chaloin [c], Kostas Kostarelos [a,b,*]

[a] Nanomedicine Lab, Faculty of Medical and Human Sciences, University of Manchester, AV Hill Building, Manchester M13 9PT, UK
[b] UCL School of Pharmacy, Faculty of Life Science, University College London, Brunswick Square, London WC1N 1AX, UK
[c] Laboratoire d'Immunologie et Chimie Thérapeutiques, CNRS, Institute de Biologie Moléculaire et Cellulaire, Strasbourg 67000, France

ARTICLE INFO

Article history:
Received 10 June 2014
Accepted 14 October 2014
Available online 24 October 2014

Keywords:
Targeted
Liposomes
Hyperthermia
Antibody
Doxorubicin

ABSTRACT

The development of actively targeted, responsive delivery vectors holds great promise for cancer therapy. Here, we investigated whether enhanced therapeutic activity of temperature sensitive liposomes (TSL) could be obtained by mild hyperthermia-triggered release of the chemotherapeutic drug doxorubicin (DOX) after hCTMO1 monoclonal antibody (anti-MUC-1) binding and uptake into cancer cells. We showed that traditional TSL (TTSL) liposome systems maintained their physicochemical and thermal properties after conjugation to hCTMO1 full IgG. Receptor-mediated cellular uptake and cytotoxic efficacy of antibody-targeted TTSL (TTSL-Ab) were investigated using 2D and 3D cell culture models. Significant enhancement in cellular uptake and cytotoxic activity after 1 h of heating at 42 °C was observed for TTSL-Ab compared to non-targeted liposomes in MUC-1 over-expressing breast cancer cells (MDA-MB-435). Tissue distribution and *in vivo* therapeutic activity were studied using different heating protocols to explore the effect of mild hyperthermia on the tumor accumulation of targeted TTSL and their therapeutic effect. Application of local, mild hyperthermia (42 °C) significantly increased the tumor accumulation of targeted TSL compared to non-targeted liposomes, associated with a moderate improvement in therapeutic activity and survival.

1. Introduction

Liposome-based chemotherapeutics is a clinically established technology offering an improved overall safety profile and reduced toxicity compared to free drugs [1]. Long circulating liposome systems have been repeatedly shown to accumulate passively at some tumor sites by the enhanced permeability and retention effect (EPR) [2]. However, their clinical therapeutic efficacy has not necessarily improved [3], mainly due to poor drug bioavailability. To enhance the efficacy of liposomal anticancer agents, two approaches have been considered extensively based on active targeting and externally triggered content release.

Contrary to passive targeting of liposomes that solely depend on the EPR effect, active targeting relies on engineering the liposome surface with targeting ligands that bind specifically to overexpressed receptors at their target site [4–7]. Considerable efforts have been made for the development of actively targeted liposomes, but their translation in the clinic is yet to be successful. One of the reasons is that their tumor accumulation is restricted by several barriers that prevent them from reaching their target cells [8,9], in addition to the need for effective content release after accumulation occurs.

Temperature-sensitive liposomes (TSL) have the advantage of controlled release of their therapeutic contents upon mild heating around the lipid bilayer phase transition temperature. ThermoDox® is a TSL containing a lysolipid, first described by Needham et al. [10], currently representing the most clinically advanced heat-responsive liposome system [11]. Recent preliminary results reported from a Phase III trial against primary hepatocellular carcinoma in combination with radiofrequency ablation [12] have shown some degree of clinical efficacy but also have already indicated that further improvements should be considered.

In order to improve the therapeutic potency of liposomal anticancer drugs, interest in developing new genres of liposome systems aim to combine the advantages of both active targeting and triggered release properties. Once bound to specific antigens on tumor cells, targeted TSL can then release their content by application of HT, either at the surface of the cells [13] or intracellularly following internalization [14,15]. Kullberg et al. [16,17] have recently reported that cytoplasmic delivery of anti-HER2 TSL can be enhanced by attaching them to the pore-forming protein, listeriolysin O. To increase the capacity of targeted TSL for intracellular delivery, multifunctional TSL have been developed by co-encapsulation of magnetic nanoparticles and doxorubicin to take the advantage of both biological targeting and physical targeting by the application of external magnetic fields [18]. Other studies have shown that potentiating intracellular content release by exposure to external HT significantly improves the cytotoxic activity of TSL [15,18].

* Corresponding author at: Nanomedicine Lab, Faculty of Medical & Human Sciences, University of Manchester, AV Hill Building, Manchester M13 9PT, UK.
E-mail address: kostas.kostarelos@manchester.ac.uk (K. Kostarelos).

http://dx.doi.org/10.1016/j.jconrel.2014.10.013
0168-3659/

Despite the promising biological activities reported *in vitro*, evaluation of targeted TSL in combination with mild HT *in vivo* has yet to be performed. The effects of HT on both targeted TSL accumulation in the tumor and drug release after intracellular uptake *in vivo* have not been previously explored.

In this study, we attempted to unravel the potential of combining monoclonal antibody-targeted TSL with local HT *in vivo*. We designed MUC-1-targeted TSL by conjugation of the clinically tested hCTMO1 mAb to the termini of "traditional" TSL (TTSL) directed against the MUC-1 antigen. Although MUC-1 is expressed on the surface of many normal epithelial cells, its expression is upregulated in the majority of epithelial cancers. On tumor cells, MUC-1 loses its apical distribution and becomes hypo-glycosylated [19]. These tumor-associated changes and cellular internalization properties by receptor recycling [20] make it an attractive candidate for cancer therapy. TTSL is a long blood circulating, temperature-sensitive liposome with the capacity to release its doxorubicin contents moderately (not abruptly) on mild heat activation [21]. TTSL have been reported to achieve high accumulation at the tumor site that can be further enhanced by HT [21–23]. Here, we hypothesized that the biological activity of TTSL liposomes could be improved by surface conjugation of anti-MUC-1 hCTMO1 IgG antibody to achieve specific binding onto cancer cells and subsequent internalization. Once inside target cancer cells, content release could be triggered by the application of HT.

To achieve these goals, we studied the tissue distribution and tumor accumulation of MUC-1-targeted TTSL (TTSL-Ab) in comparison to non-targeted TTSL using the MDA-MB-435 xenograft model. We applied different therapeutic protocols by varying the timing and sequence between HT and injection of liposomes to also allow HT to vasodilate tumor vessels and increase TTSL tumor accumulation. Our *in vivo* investigations were also designed with and without application of a second mild HT session at 24 h after intravenous administration to trigger liposomal drug release after maximum tumor accumulation. Moderate improvement in the biological activity and survival was observed from TTSL-Ab with a second HT, compared to non-targeted TTSL. Our results suggested that targeted TTSL in combination with mild HT can offer new opportunities in the development of advanced cancer therapeutics.

2. Results

2.1. Preparation and characterization of MUC-1 TTSL-Ab liposomes

hCTMO1 Ab conjugation to TTSL liposomes was performed by the post-insertion method that is based on the translocation of DSPE-PEG_{2000}-Ab micellar lipids in exchange with liposomal bilayers [24]. In this way, the Ab ligand will be presented at the outer surface of the liposomes and maintain its binding capacity [25]. Briefly, mal-DSPE-PEG_{2000} Ab micelles were prepared by conjugation of thiolated Ab (Ab-SH) with maleimide (mal)-DSPE-PEG_{2000} micelles (Fig. S1A). Conjugation was confirmed by an upper shift of the anti-MUC-1 Ab band on SDS–PAGE (band 3), indicating an increase in its molecular weight after conjugation (Fig. S1B). In order to determine the best post-insertion temperature, post-insertion was done at three different conditions; 60 °C (1 h), 45 °C (1 h) and 39 °C (5 h) (Fig. S2A). The amount of antibody post-inserted into TTSL liposomes was then determined in each elution fraction by quantification of both Ab using BCA assay and lipids using the Steward assay (Fig. S2B). The optimum post-insertion efficiency was obtained after 1 h incubation at 60 °C, evidenced by co-localization of mal-DSPE-PEG_{2000} Ab micelles with the liposome fraction (Fig. S2B).

The amount of Ab conjugation obtained was 13 μg Ab/μmol lipid at Ab: lipid 1:1000 molar ratio and 26.5 μg Ab/μmol lipid at Ab: lipid 1:500 molar ratio. SPR was used to check the integrity of the anti-MUC-1 antibody (Ab) after conjugation to TTSL liposomes. SPR sensorgrams of mal-DSPE-PEG_{2000} Ab micelles and TTSL-Ab indicated that the antibody conserved its binding capacity in a concentration-dependent manner (Fig. S3). Interestingly, we observed that the equilibrium dissociation constant of Ab after conjugation to liposomes was lower than the Ab itself indicating higher binding affinity (Fig. S3D).

No significant change in the size of liposomes was observed after Ab conjugation. Both TTSL and TTSL-Ab liposomes were slightly larger than 100 nm in size with low polydispersity index. Moreover, DOX was successfully encapsulated (>90%) without affecting the particle size of the liposomes (Fig. 1B). A decrease in zeta potential (surface charge) was observed after Ab conjugation and the reduction was proportional to the amount of the Ab conjugated, in agreement with other previous studies [26,27].

2.2. DOX release studies

Serum stability and thermal responsiveness of TTSL and TTSL-Ab liposomes were studied by quantifying the amount of encapsulated DOX release at 37 °C and 42 °C, respectively. No significant leakage of DOX from both TTSL and TTSL-Ab was observed after incubation for 60 min in 50% serum at 37 °C (Fig. 1Ci). At 42 °C rapid release of DOX was obtained (>80%) after 1 min incubation from TTSL liposomes with and without Ab (Fig. 1Cii). DOX release data showed that TTSL-Ab liposomes maintained their serum stability and temperature sensitivity after Ab conjugation.

2.3. Cellular binding of anti-MUC-1 antibody

We then tested the expression of MUC-1 antigen in various human cancer cell lines (MDA-MB-435, MCF-7 and C33a) (Fig. S4A). MDA-MB-435 and MCF-7 cell lines were found MUC-1 positive, whereas C33a cells were considered negative to MUC-1 as no binding of Cy3 antibody was observed under the experimental conditions tested. The binding capacity of anti-MUC-1 Ab after each step of conjugation to TTSL liposomes was studied by examining affinity towards MDA-MB-435 cells using immunostaining with Cy3-labeled secondary antibody and visualization with confocal microscopy (Fig. S4B). Binding data confirmed that the antibody maintained its activity after incorporation into TTSL liposomes, in contrast to complete loss of binding after 1 h incubation at 80 °C.

2.4. Cellular Uptake of TTSL and TTSL-Ab

The cellular uptake of TTSL-Ab liposomes and their internalization into MUC-1 + ve cells was studied next by confocal microscopy (Fig. 2). The cellular uptake of both the lipids (DiI; white channel) and the encapsulated drug (DOX; red channel) after 1 h and 3 h incubation with cells were enhanced by the anti-MUC-1 Ab. In comparison, only moderate cellular uptake was observed from non-targeted TTSL (DiI signal) after 3 h incubation, presumably through non-specific endocytosis. No internalization of TTSL without targeting ligand was observed based on DOX fluorescence, further indicating the poor levels of cellular uptake compared to targeted TTSL (amount of DOX internalized close to background levels) (Fig. 2B).

The kinetics of cellular uptake were also studied by imaging DOX-loaded TTSL and TTSL-Ab (Fig. S5) at different time points. Rapid binding and internalization of TTSL-Ab liposomes into MDA-MB-435 cells was observed as early as 1 h after incubation, which increased further over 24 h. Cellular uptake can be further enhanced by increasing the density of anti-MUC-1 antibody per liposome from 13 μg Ab/μmol lipid to 26.5 μg Ab/μmol lipid in TTSL-Ab-I and TTSL-Ab-II, respectively (Fig. S5). The enhancement in cellular uptake was specific to MUC-1 + ve cells since no significant difference was observed in internalization within C33a cells (MUC-1-ve).

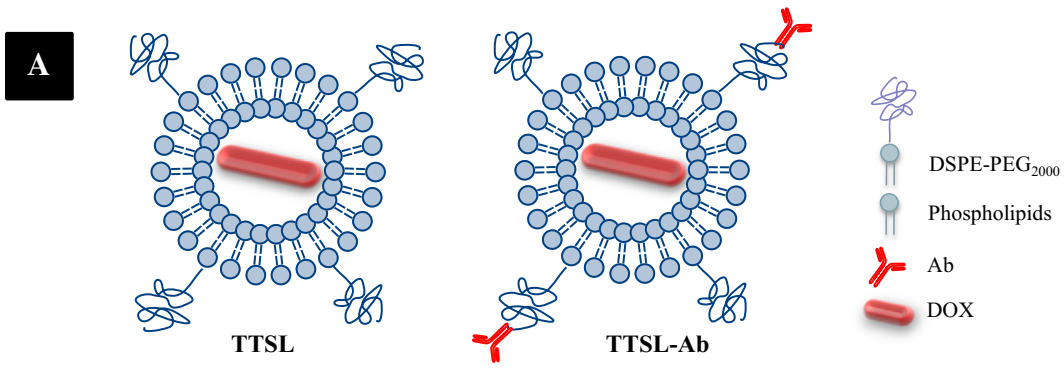

B

Liposome	Ab/ µg/µmol	Size (nm)	Polydispersity Index (PDI)	Loading (nm)	Zeta (mV)
TTSL	-	127.6 ± 2.1	0.07 ± 0.008	129.4 ± 2.1	-15.3 ± 1.6
TTSL-Ab-I	13.0	130.1 ± 1.3	0.04 ± 0.005	127.6 ± 1.4	-20.3 ± 2.5
TTSL-Ab-II	26.5	128.2 ± 1.6	0.08 ± 0.006	126.5 ± 1.3	-28.0 ± 0.8

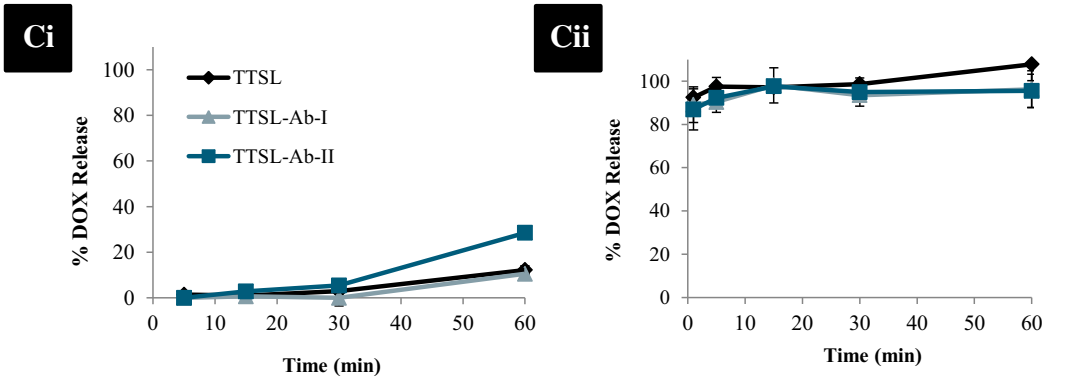

Fig. 1. Design and characterization of TTSL and TTSL-Ab. (A) Schematic presentation of non-targeted TTSL and targeted TTSL-Ab. (B) Size, PDI, and surface properties of TTSL before and after post-insertion of MUC-1 antibody at two different ratios. (Ci) DOX release from TTSL and TTSL-Ab liposomes after incubation at 37 °C. (Cii) DOX release after heating at 42 °C. DOX release experiments were performed in 50% CD-1 mouse serum to simulate physiological conditions. Data are presented as mean ± STD ($n = 3$).

2.5. Cytotoxic activity of DOX-loaded TTSL and TTSL-Ab

To evaluate the cytotoxic activity of targeted TTSL-Ab compared to TTSL, cellular viability was measured using the MTT assay in both MUC-1 + ve and MUC-1-ve cell lines with and without exposure to HT. To ensure that DOX was becoming bioavailable intracellularly, mild HT was applied to trigger release from liposomes after cellular uptake. Limited cytotoxic activity (~90% cell viability) was observed from cells treated with TTSL-Ab without exposure to HT. In comparison, intracellularly triggered DOX release from targeted TTSL-Ab liposomes in MDA-MB-435 (MUC-1 + ve) cells resulted in significant ($p < 0.01$) enhancement in cytotoxicity compared to that without heating (only 60% cell viability) (Fig. 3A). The observed cytotoxic effect was also dependent on the density of anti-MUC-1 antibody conjugation to liposomes. These data was in agreement with the cellular uptake findings above and indicated that although some spontaneous release of DOX could occur after TTSL-Ab internalization, the intracellular bioavailability, therefore activity, of the drug molecules can be significantly enhanced by triggering its release with HT. No cytotoxic activity was observed from non-targeted TTSL with and without HT. Also, both targeted and non-targeted TTSL did not have any cytotoxic activity on C33a (MUC-1-ve) cells, which further confirmed the selective (for MUC-1 expressing cells) activity of targeted TTSL (Fig. 3B). In comparison, free DOX showed the highest cytotoxic activity on both cell lines because of the rapid uptake of drug by the cells in its free from.

2.6. Localization and Cytotoxic Activity of TTSL and TTSL-Ab in Multicellular Spheroids (MCS)

The therapeutic efficacy of targeted TTSL-Ab liposomes will depend not only on their cell receptor binding and internalization, but also on their ability to travel deeper within the tumor interstitium. MCS were used to better mimic the avascular regions of the tumor tissue. MCF-7 (MUC-1 + ve) MCS were used in these studies instead of MDA-MB-435 due to the inability of the latter to form MCS. TTSL-Ab-II showed better cellular uptake and cytotoxic activity compared to TTSL-Ab-I, therefore this system was selected for further studies using MCS and *in vivo*. MCF-7 MCS were treated with DOX-loaded TTSL and TTSL-Ab and compared to free DOX. After 24 h incubation at 37 °C, liposomes were removed and MCS were washed with PBS while DOX localization (DOX signal at 535–674) was assessed by confocal laser scanning microscopy (Fig. S6A). No significant enhancement in the fluorescence

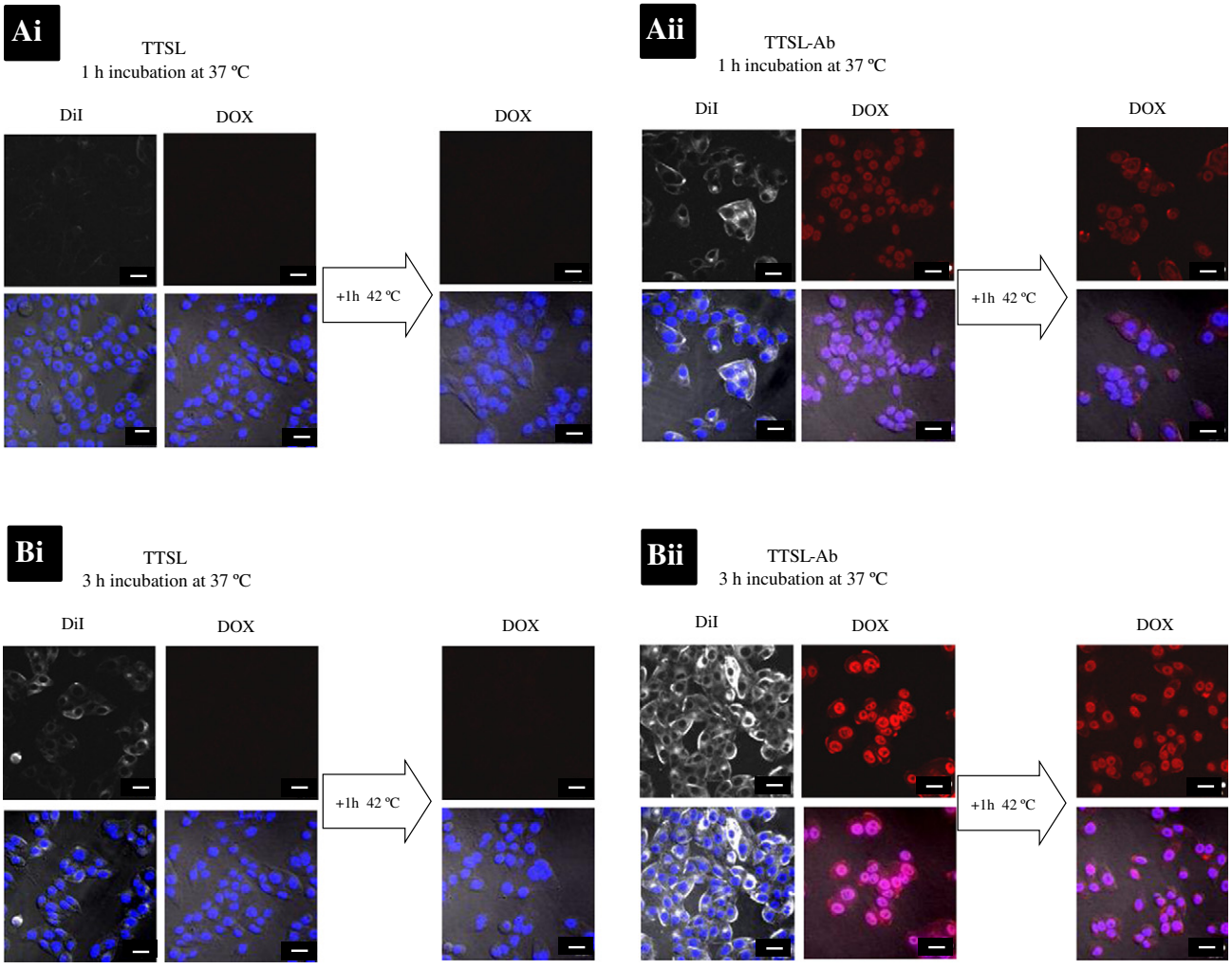

Fig. 2. Cellular uptake studies of TTSL and TTSL-Ab into MDA-MB-435 cells. Confocal microscopy imaging of monolayer of MDA-MB-435 cells (MUC-1 + ve) showed the uptake of DiI-labeled and DOX encapsulated TTSL and TTSL-Ab (26 μg Ab/μmol lipid) after (Ai and Aii) 1 h and (Bi and Bii) 3 h incubation. White channel represents the uptake of DiI-labeled liposomes. Red channel represents DOX before and after 1 h heating at 42 °C. Co-localization with DAPI stain (blue channel) of the nucleus is shown in the overlay images. Top images are fluorescence images from excitation of DiI (left) and DOX (centre and right). Bottom images represent the overlay with DAPI and bright field images. Scale bar is 20 μm. DiI was imaged at 514 nm laser excitation source and 585 nm output filter. DOX fluorescence signal was detected at 488 nm laser excitation source and 535–674 nm output filters.

intensity of DOX was observed from TTSL-Ab compared to TTSL that can be due to limited capacity of these liposomes to transport deeper into MCS. A moderate increase in DOX penetration was observed from TTSL-Ab after 15 min heating at 42 °C.

The cytotoxic activity of the targeted TTSL-Ab was compared to TTSL by evaluation of tumor spheroid growth retardation. Fig. S6B shows the optical microscopy images of MCF-7 spheroids over time under standard cell culture conditions. Both TTSL and TTSL-Ab significantly

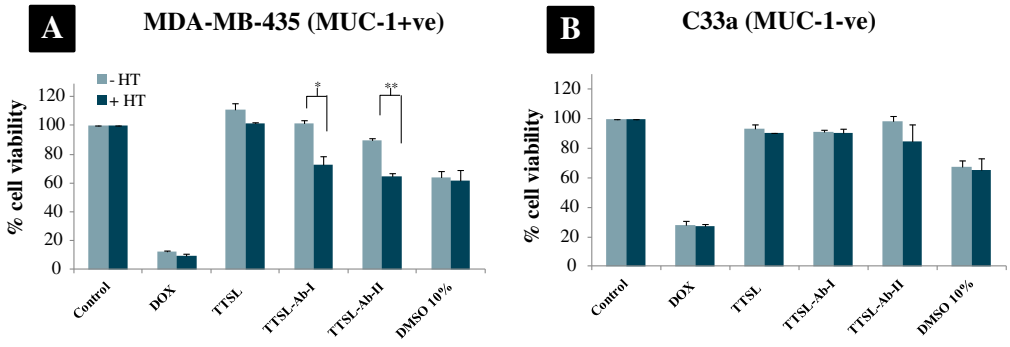

Fig. 3. MTT assay of TTSL and TTSL-Ab. (A) MDA-MB-435 and (B) C33a cells. Cellular monolayers were treated with TTSL and TTSL-Ab at 10 μM DOX concentration for 3 h at 37 °C. After 3 h incubation, the liposomes containing media were removed and replaced with fresh media. To test the effect of heat trigger release, cells were incubated at 42 °C (1 h, in CO_2 incubator) and compared to no heating condition. MTT assay was performed 48 h after treatment and expressed as percentage of cell viability. Results represent average ± STD of at least 2 independent experiments (6 wells per treated group). $^{*}p < 0.05$ and $^{**}p < 0.01$.

retarded spheroid growth compared to control (at day 22 $p < 0.05$ and $p < 0.001$, respectively). Spheroid growth retardation observed for TTSL-Ab was comparable to free DOX, in both cases normalized spheroid volume was less than double after 22 days post-treatment (Fig. S6C).

Targeted TTSL-Ab with and without HT showed greater control on MCS growth compared to non-targeted TTSL. Although DOX penetration into MCS from TTSL and TTSL-Ab was not significantly different, the enhancement in spheroid growth retardation was thought to indicate increased DOX release able to restrict MCS proliferation and growth (Fig. S6C). Although free DOX showed the highest MCS growth retardation *in vitro*, this effect is not representative of *in vivo* conditions because free DOX is eliminated rapidly from the blood compartment offering minimal interaction with tumor cells.

2.7. Tissue Distribution of Intravenously Administered TTSL and TTSL-Ab

The pharmacological behavior of targeted TTSL-Ab was then studied *in vivo*. We designed these studies in order to determine the effect of localized HT on the ensuing drug bioavailability within the tumor and the impact of triggering drug release. Tissue distribution was determined by comparing three different heating protocols (Scheme 1). In each protocol two heating sessions were applied. The purpose of the 1st HT was to increase drug accumulation via HT-mediated tumor vasodilatation [28]. The 2nd HT aimed to release the drug interstitially following accumulation of liposomes inside the tumor tissue. The *in vivo* therapeutic efficacy of the targeted TTSL-Ab was then compared to non-targeted TTSL.

First, we studied the blood circulation profile of TTSL and TTSL-Ab due to the importance of prolonged blood circulation on the level of tumor accumulation [29]. Fig. 4 showed that both TTSL and TTSL-Ab exhibited prolonged DOX circulation half-life, irrespective to the HT protocol applied. This suggested that conjugation of anti-MUC-1 Ab on the TTSL surface did not compromise their blood circulation time. TTSL-Ab contained 26.5 μg Ab/μmol lipid (equivalent to 15 Ab molecules per liposome) and according to previous studies grafting of MUC-1 antibody at this density should not interfere with blood circulation [20].

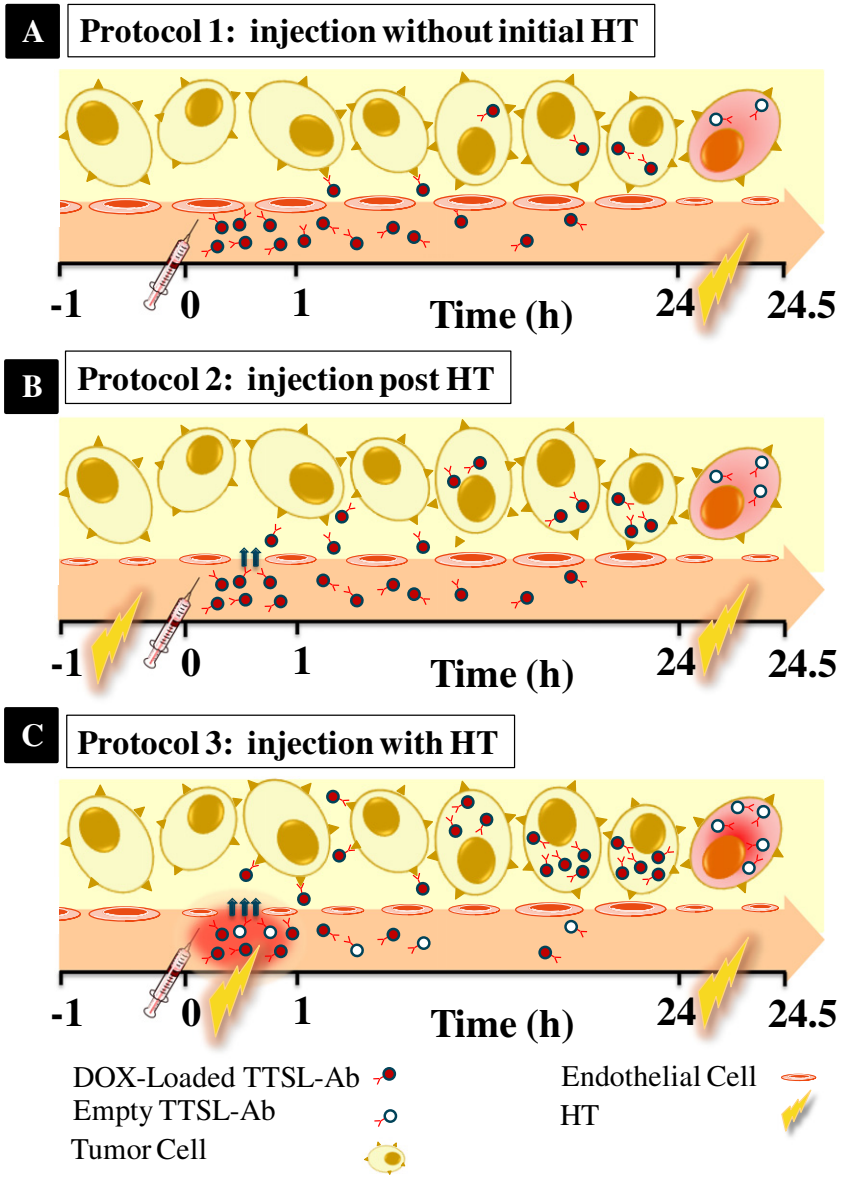

Scheme 1. Schematic presentation of the three HT protocols studied. The three heating protocols different based on the timing of liposome injection in relation to the initial HT (for 60 min). (A) Liposomes were injected without application of initial HT; (B) liposome injection immediately after local HT was applied at the tumor area; and (C) liposomes were injected first and local HT of the tumor was performed immediately after injection. A 2nd localized HT session (30 min) was applied 24 hours after liposome injection in all three protocols in an attempt to trigger drug release from liposomes that had accumulated in the tumor.

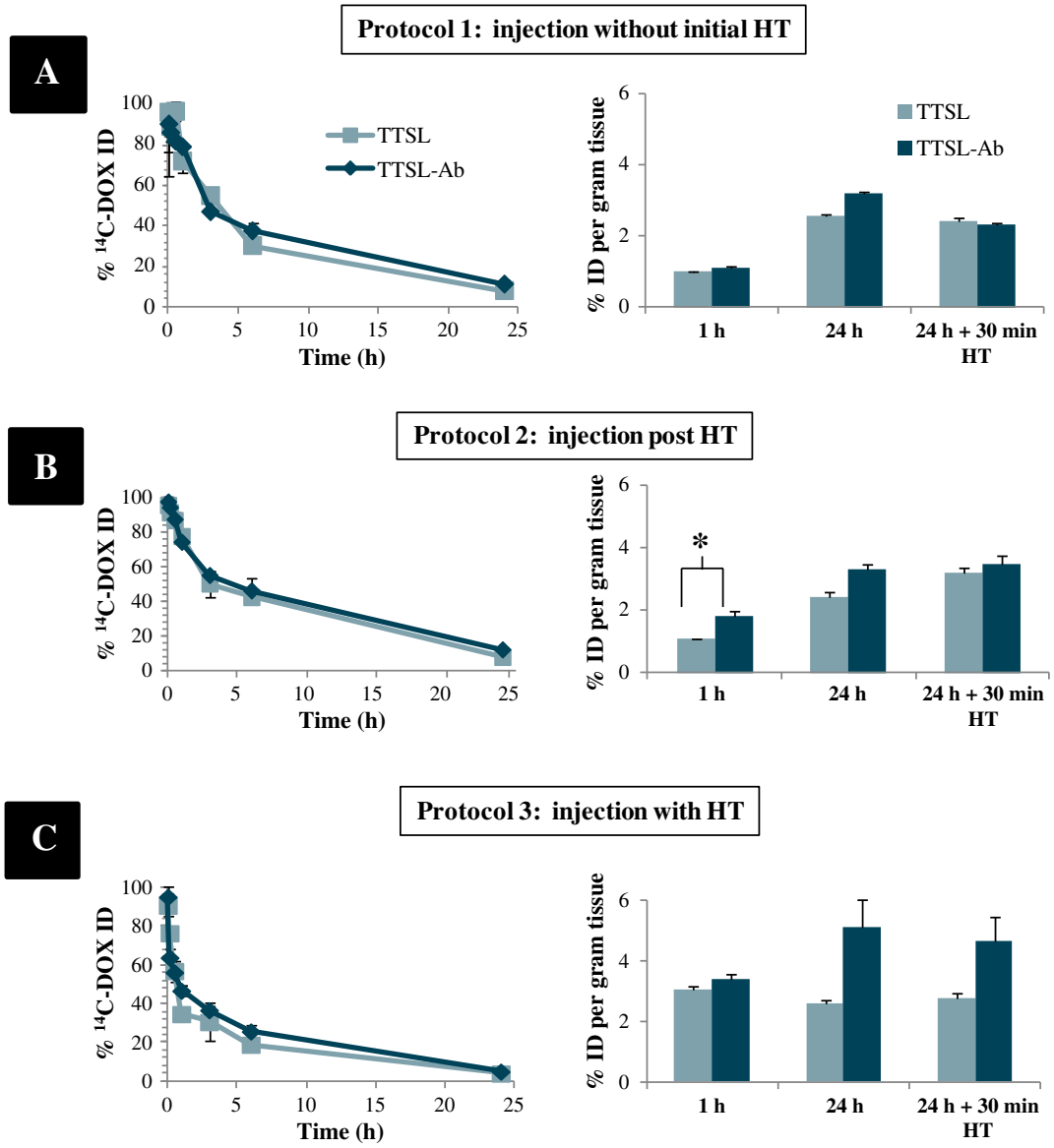

Fig. 4. Blood profile and tumor accumulation of TTSL and TTSL-Ab. TTSL and TTSL-Ab were injected intravenously into MDA-MB-435 (MUC-1 + ve) tumor-bearing athymic nude mice by application of the three heating protocols (described in Scheme 1). Blood profile data and tumor accumulation (left) of ^{14}C-DOX are shown for (A) liposome injection without initial HT; (B) liposome injection after initial HT (tumor was heated for 1 h at 42 °C prior to injection); and (C) liposome injection first, followed by immediate tumor HT for 1 h at 42 °C. Data are presented as mean ± SEM (n = 3–4). *p < 0.05.

The shortest blood circulation profile was obtained with Protocol 3, due to drug release in the tumor vasculature as the 1st HT session was applied simultaneously with liposome injection. On the other hand, in the other two protocols the liposome injection was either performed in the absence of the 1st HT (Protocol 1) or immediately after (Protocol 2).

Comparison between the ^{14}C-DOX tumor levels from TTSL and TTSL-Ab indicated almost identical values without initial HT (Protocol 1) at all time points studied (Fig. 4A). Interestingly, TTSL-Ab injected post-HT (protocol 2) resulted in higher tumor accumulation compared to TTSL liposomes 1 h after injection ($p < 0.05$) (Fig. 4B). Similar increase in ^{14}C-DOX within the tumor by TTSL-Ab was also observed in the case of injections with HT (protocol 3) (Fig. 4C). The highest tumor accumulation was achieved from Protocol 3 resulting in almost 2- to 3-fold increase in ^{14}C-DOX compared to the other two protocols

The effect of antibody conjugation on the tissue biodistribution of TTSL and TTSL-Ab along with the impact of the different heating protocols was also evaluated (Fig. S7). Due to triggered drug release during Protocol 3, higher levels of ^{14}C-DOX were detected in the tissues as early as 1 h after injection. This effect was observed in liver, kidney and heart, we believe due to early release of free drug in blood circulation. Quantification of ^{14}C-DOX levels in different organs 24 h before and after application of the 2nd HT session showed the opposite effect. The accumulation of ^{14}C-DOX across all tissues was generally higher after treatment with Protocols 1 and 2. We believe this was due to their longer circulation without release of DOX. Tissue distribution of DOX from TTSL and TTSL-Ab was almost identical with some increase in the spleen and liver accumulation with TTSL-Ab. This finding agreed with previous studies [30,31] and indicated capture of vesicles in the filtering apparatus of these organs.

To further validate the ^{14}C-DOX tissue distribution data, TTSL and TTSL-Ab administration under the three HT protocols was followed by whole-body optical imaging of DOX fluorescence 1 h and 24 h after injection (before and after 2nd HT) using an IVIS camera (Fig. 5). In agreement with ^{14}C-DOX tissue distribution, IVIS imaging showed that Protocols 1 and 2 were associated with higher DOX signals throughout the body. This was more obvious with the TTSL-Ab compared to TTSL

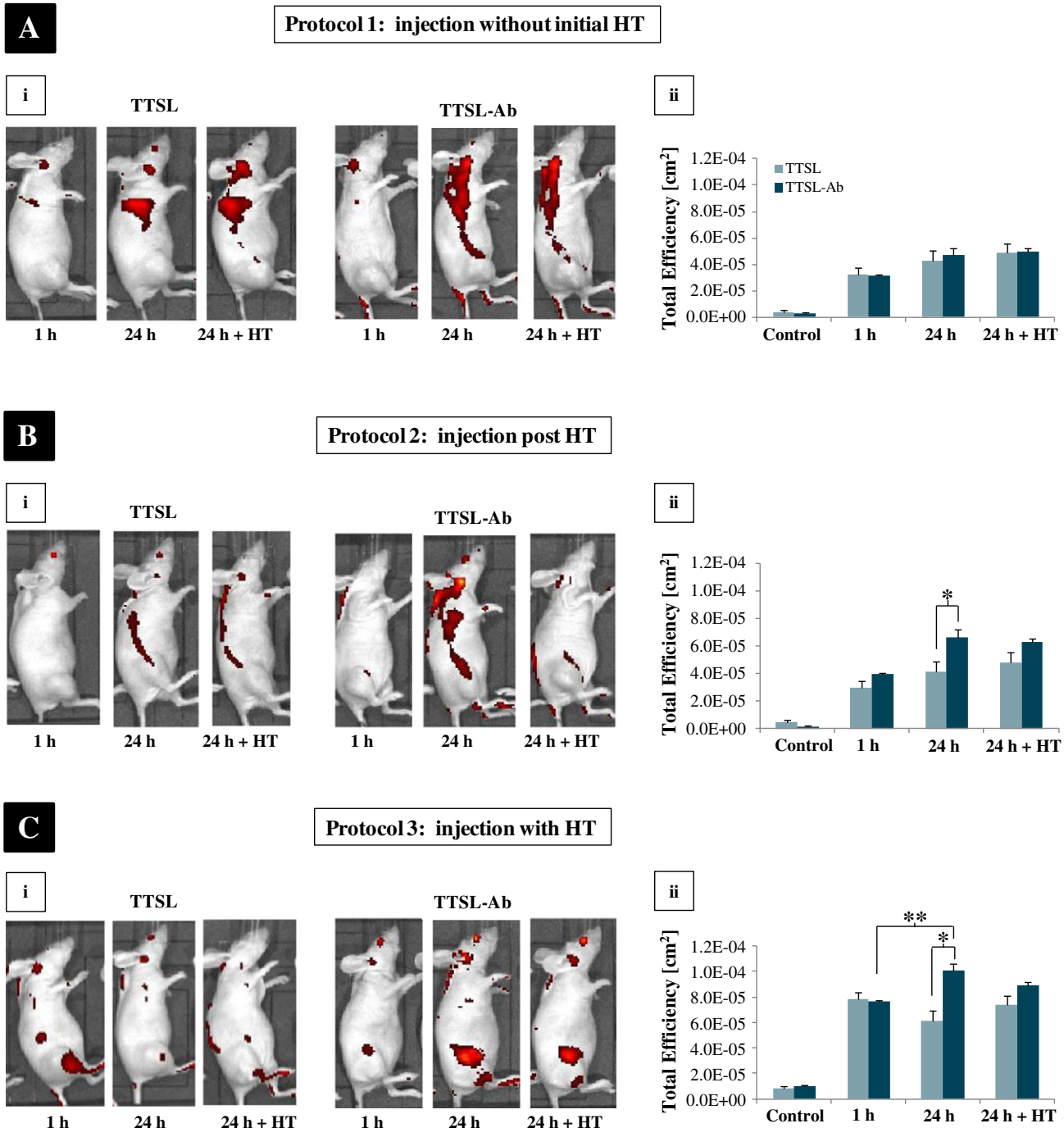

Fig. 5. Whole-body imaging of athymic nude mice after injection with TTSL and TTSL-Ab. Live fluorescence imaging of DOX-loaded TTSL and TTSL-Ab injected mice by application of the three heating protocols using the IVIS Lumina II imaging system. (Ai, Bi, and Ci) Live fluorescence imaging. (Aii, Bii, and Cii) DOX fluorescence intensity signal quantification at 500 nm/DsRed excitation and emission filters from the tumor expressed as average ± SEM. In the first two HT protocols, the high background signal from DOX accumulation into vital organs limited the signal of DOX in the tumor under this imaging scale used. Control group was animals that received single HT treatment only.

(Fig. 5Ai and Bi). Total DOX fluorescence intensity levels at the tumor site showed that the TTSL-Ab resulted in significantly higher tumor accumulation using Protocols 2 and 3 only (Fig. 5Bii and Cii) as was the case with ^{14}C as well.

2.8. Tumor growth retardation and survival

The biodistribution data above indicated a 2-fold increase in tumor uptake of the targeted TTSL-Ab compared to TTSL. The highest DOX accumulation was achieved by application of Protocol 3 (liposome injection simultaneously with an initial HT session). Therefore, we decided to take this heating protocol forward for evaluation of the therapeutic activity of TTSL-Ab. MDA-MB-435 tumor-bearing nude mice were treated with both TTSL and TTSL-Ab, with and without application of a 2nd HT session (at 24 h post-vesicle injection). Tumor growth retardation (Fig. 6A) indicated that injection with both TTSL and TTSL-Ab loaded with DOX showed significant growth retardation compared to untreated animals. On days 30 and 34, the treatment groups TTSL + 2nd HT, TTSL-Ab and TTSL-Ab + 2nd HT resulted in significant tumor growth retardation compared to the control group (received single HT

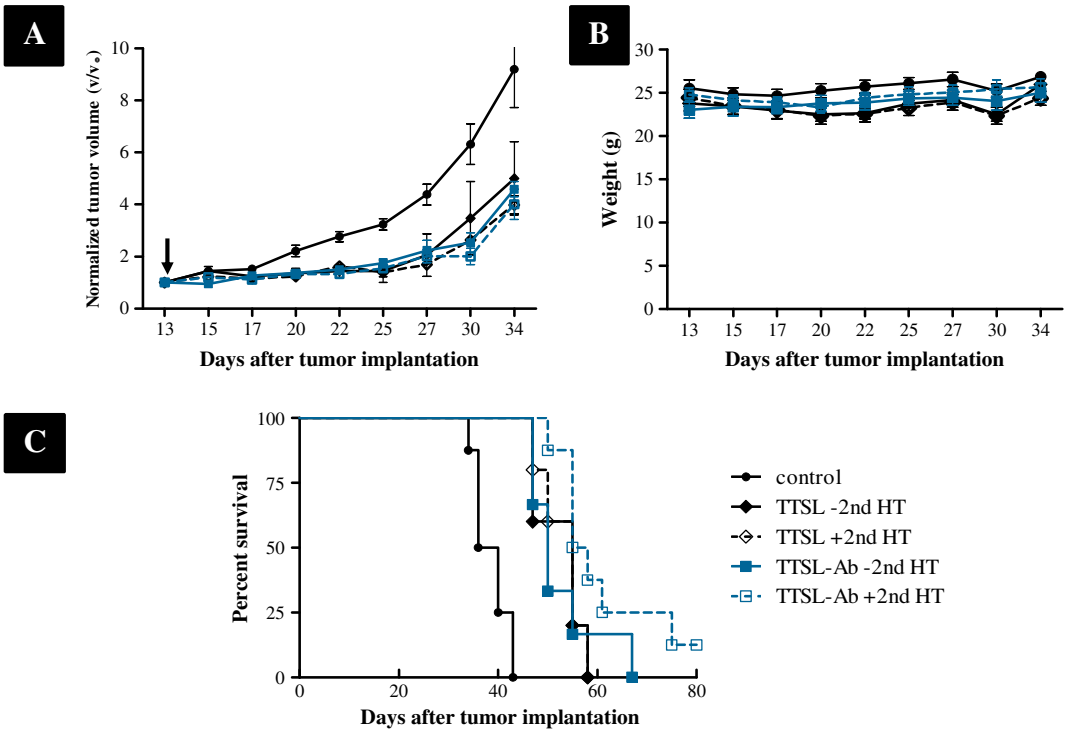

D

Treatment	Dose (mg/kg)	Mean survival time (days)	Increase in life span (%)[a]	Significance (p) vs control
Intravascular release protocol (injection with HT)				
Control	-	36.0	0	-
TTSL -2nd HT	1 × 5	55.0	+45.0	0.0010
TTSL +2nd HT	1 × 5	55.0	+45.0	0.0010
TTSL-Ab-II -2nd HT	1 × 5	50.0	+32.0	0.0027
TTSL-Ab-II +2nd HT	1 × 5	56.5	+49.0	<0.0001

[a] % of increase in life span = mean survival time of treated / mean survival of control × 100 -100.

Fig. 6. *In vivo* tumor growth delay and survival studies. MDA-MB-435 tumor-bearing mice treated with TTSL and TTSL-Ab liposomes applying (protocol 3) with and without 30 min 2nd HT 24 h after injection. (A) Normalized tumor volume. A one-way ANOVA followed by Tukey's multiple comparison tests indicated significant tumor growth retardation of treated mice compared to control. At day 30, the *p* values of control vs TTSL + 2nd HT, control vs TTSL-Ab − 2nd HT, and control vs TTSL-Ab + 2nd HT were <0.05, <0.01, and <0.001, respectively. At day 34, the *p* values of control vs TTSL + 2nd HT, control vs TTSL-Ab − 2nd HT and control vs TTSL-Ab + 2nd HT were <0.05, <0.05, and <0.01, respectively. (B) Body weight and (C) survival curves following single administration. Therapy started on day 13 after implantation with average tumor size of 100 mm^3. Animals were injected intravenously with TTSL and TTSL-Ab at 5 mg/kg DOX followed by immediate 1 h HT. Control animals were not injected, and treated with a single session of HT. Each group ($n = 5–7$, average ± SEM). (D) Survival analysis of MDA-MB-435 tumor-bearing mice treated with DOX-loaded TTSL and TTSL-Ab.

treatment only). However, no statistical significance was observed between those treatment groups. All treated animals did not show any signs of toxicity, abnormal behavior or any significant fluctuation in body weight (Fig. 6B). The survival curves indicated that highest increase in life span was obtained from treatment with TTSL-Ab accompanied with a 2nd HT session compared to the other treatment groups (Fig. 6C). All treatment groups displayed significantly prolonged survival ($p < 0.001$) compared to the untreated group (Fig. 6D).

3. Discussion

Liposomes can enhance the localization of cytotoxic agents in some solid tumors and decrease drug uptake by sensitive organs [1]. Next-generation liposome systems are envisioned to possess active targeting and triggered drug release capabilities [18]. Several types of actively targeted liposomes have been developed with increased cellular uptake; however, none of them have been successfully translated to the clinic [9]. Despite the increase in specific cellular uptake and cytotoxic activity from targeted liposomes *in vitro* [32,33], only some studies have reported enhanced tumor accumulation *in vivo*, such as in the case of 2C5-Doxil-targeted liposomes [34]. Also, previous work using mAb-targeted liposomes has shown no improvement in overall accumulation within solid tumors [8,35–37]. We believe the reason for such results is because tumor accumulation for both targeted and non-targeted pegylated liposomes is dominated by the vascular architecture and leakiness of the tumor (depends on the density of the pericytes and smooth muscle cells that cover the blood microvessels), allowing operation of the EPR effect. Even in the case of extravasation through the tumor vasculature, targeted liposomes face a number of barriers to transport through in tumor interstitium before reaching their potential cellular targets. These factors are in most cases tumor-type specific, including the density by which tumor cells pack, the biochemical consistency of the tumor extracellular matrix, and the build-up of high interstitial fluid pressure. The only cases in which mAb-targeted liposomes have shown better tumor accumulation than their non-targeted counterparts is in very rapidly growing tumors, where

tumor cells are growing immediately adjacent to vasculature [9]. However, even in these cases tumor accumulation will be dependent on vascular extravasation in addition to the "binding site barrier" effect [38].

The ability of antibody-targeted liposomes to be internalized by cells can result in improvements in drug bioavailability, especially for drugs acting against intracellular targets [39]. Kirpotin et al. showed similar overall tumor accumulation levels for both anti-HER2-targeted and non-targeted liposomes [8,37]. However, the intra-tumoral microdistribution and cellular localization of targeted anti-HER2 liposomes were different due to their cellular internalization capacity. Significant portion of HER2-targeted liposomes was observed within cancer cells compared to non-targeted liposomes mainly found in stromal cells [8]. Similarly, transferrin-targeted oxaliplatin liposomes showed significant tumor growth control in comparison to non-targeted liposomes as a result of intracellular drug transport into the cytoplasm of colon 26 tumor cells by transferrin receptor-mediated internalization [40].

An alternative strategy is to design-targeted liposomes against endothelial cells. Examples of that include the RGD [36] and NGR [41] targeted liposomes directed against different integrins ($\alpha\nu\beta3$ and $\alpha5\beta1$) or against the aminopeptidase N (CD13) receptor on angiogenic endothelial cells. Endothelial cell-targeted liposomes carrying doxorubicin increased tumor accumulation [41] and showed control over tumor growth and survival [36,41]. Similarly, therapeutic effects have been reported for targeted liposomes directed against micrometastases [20] or blood-borne cancers [33], such as those with an affinity towards B cell lymphoma, overexpressing CD19 surface antigens [33]. In this case, the role of liposome internalization was not significant. The therapeutic activities obtained from targeted liposomes encapsulating doxorubicin or vincristine and directed towards CD19 (internalizing) antigen or against CD20 (non-internalizing) antigen were dependent on the type of drug rather than its internalization ability [42]. The faster release rate of vincristine from anti-CD20 liposomes compared to doxorubicin explained improved therapeutic activity observed even without internalization [42]. In addition, different approaches have been investigated in an attempt to increase the penetration of both liposomes and antibody-targeted liposomes into solid tumors. One approach involved the use of the extracellular matrix (ECM) degrading enzyme, hyaluronidase, prior to liposome administration [43] or X-ray irradiation that also acted against ECM integrity [44].

HT is a well-established method to augment liposomal accumulation into solid tumors [21,45]. Dewhirst and colleagues observed significant enhancement in the extravasation of liposomes, monoclonal antibodies, and antibody fragments into solid tumors by the application of mild HT [46–49]. This enhancement of tumor accumulation by HT is due to increases in local blood flow [50], a reported 40%–60% increase at 41 °C, resulting in increased microvascular permeability [28,49,51]. Interest in designing receptor-targeted liposomes with temperature sensitivity has increased, with some previous studies showing cell-specific cytotoxic activity after heating *in vitro* [15,18]. Whether such findings hold *in vivo* in preclinical tumor models by triggering intracellular drug release after tumor accumulation was one of the aims of this study.

The combinatory functionality of targeting and temperature sensitivity was designed in anti-MUC-1-targeted TSL (TTSL-Ab) liposomes that have the potential to internalize specifically into tumor cells and offer on-demand drug release in response to mild HT. The TTSL liposomes were chosen for their long blood circulation and substantial accumulation in the tumor when combined with moderate HT (<42 °C). Previously, we have shown that TTSL administration into B16-F10 tumor-bearing mice in combination with mild HT could result in dramatic increases in tumor drug accumulation 24 h after administration and heat application [23]. This finding was a result of three factors: (a) prolonged blood circulation, (b) the stability of TTSL, and (c) the enhanced tumor extravasation following HT. We hypothesized that the therapeutic activity of TTSL can be further improved by conjugation of anti-MUC-1 antibodies to increase their binding specificity and cellular internalization, followed by content release inside the tumor cells triggered by application of mild HT.

In this study, anti-MUC-1 TTSL-Ab was successfully prepared by post-insertion of anti-MUC-1 mal-DSPE-PEG_{2000} micelles into preformed TTSL. TTSL-Ab liposomes retained their characteristics, drug-loading capacity, and thermal-responsiveness that agreed with previously described targeted TSL [14,52]. In addition to specifically increasing cellular uptake and cytotoxicity to MDA-MB-435 (MCU-1 + ve) cells after exposure to HT *in vitro*, the potential of targeted TTSL-Ab was evaluated *in vivo*. Liposome encapsulated ^{14}C-DOX accumulated in the tumor following TTSL-Ab injection after or during HT application that was thought to be due to improvements in tumor penetration induced by local HT. On the contrary, our results showed that both non-targeted TTSL and targeted TTSL-Ab accumulated to the same extent when injected without application of an initial HT session, similar to what was observed in other studies because of their similar penetration into the tumor [8]. The observed intratumoral increase of ^{14}C-DOX from TTSL-Ab is thought to be a result of enhanced retention of the liposomes. Active binding and internalization via the receptors on MDA-MS-435 tumor cells allowed them to be retained in the tumor for a longer time and prevented them from being washed out of the tumor vasculature and back into systemic circulation [9]. Application of 30 min mild HT to trigger drug release from accumulated liposomes 24 h after injection did not significantly change drug levels in the tumor or efficacy. Similar findings were observed from *in vivo* imaging and confirmed the above organ distribution and tumor accumulation data. Significant increase in DOX tumor accumulation was achieved from TTSL-Ab when HT was combined with injection (Protocols 2 and 3) compared to TTSL ($p < 0.05$).

Despite the two-fold increase in tumor uptake of TTSL-Ab liposomes compared to TTSL, only modest improvement in tumor growth retardation and survival was achieved compared to TTSL with and without application of a 2nd HT session. Similar moderate improvements in therapeutic efficacy have been observed previously by triggering intracellular release after tumor accumulation using pH-sensitive anti-HER2-targeted liposomes [53]. The reason for such data was thought to be primarily due to insufficient bioavailable tumor drug concentration after single injection to control tumor growth. We may therefore, suggested that the therapeutic activity of TTSL-Ab developed here can be optimized after repeated administration.

Targeted, temperature-sensitive DOX-loaded liposomes (TTSL-Ab) have been successfully developed and studied thoroughly as cancer thermo-chemotherapeutics. TTSL-Ab maintain their physicochemical and structural integrity with stable retention of the drug and their thermal properties after grafting of antibodies. The role of mild HT as an effective modality to increase the therapeutic specificity and augment drug accumulation in the tumor has also been illustrated. These results have implications for other actively targeted drug delivery systems and can instruct on the challenges around the design of therapeutically efficacious multi-modal vesicle systems.

4. Experimental methods

4.1. Chemicals and reagents

hCTMO1; anti-MUC-1 IgG mAb, and other chemicals are described in details in SI text.

4.2. Cell lines

Details of the cell lines used are explained in SI text.

4.3. Preparation of TTSL liposomes

Non-targeted TTSL (25 mM) composed of DPPC:HSPC:CHOL:DSPE-PEG_{2000}; 54:27:16:3 mol/mol% were prepared by thin film hydration

method followed by extrusion as explained before (details of the preparation method can be found in SI text). Liposome size and surface charge were measured by using Zetasizer Nano ZS (Malvern, UK).

4.4. Preparation of targeted TTSL (TTSL-Ab): conjugation of anti-MUC-1 antibody to DSPE-PEG$_{2000}$ maleimide micelles

For the preparation of targeted TTSL-Ab liposomes, TTSL liposomes (25 mM) composed of DPPC:HSPC:CHOL:DSPE-PEG$_{2000}$; 54:27:16:3 mol/mol% were first prepared as mentioned earlier followed by post-insertion of anti-MUC-1 mal-DSPE-PEG$_{2000}$ micelles using the previously described procedure with slight modifications [54]. Details of the chemical conjugation of anti-MUC-1 antibody to DSPE-PEG$_{2000}$ Maleimide micelles are as explained in the SI text.

4.5. Post-insertion of DSPE-PEG$_{2000}$ maleimide micelles into TTSL liposomes

Mal-DSPE-PEG$_{2000}$ Ab micelles were then post-inserted into preformed TTSL liposomes at two different Ab: lipids molar ratios (1:500 and 1:1000) by 1 h incubation at 60 °C. TTSL-Ab liposomes were then separated from non-incorporated mal-DSPE-PEG$_{2000}$ Ab micelles by using Sepharose CL-4B column in HBS (pH 7.4). Post-insertion efficiency was determined by collecting elution fractions (1 ml each) and analyzed spectrophotometrically for the presence of Ab (BCA protein assay, at 562 nm) [55] and liposomes (Stewart's assay, at 485 nm), using Cary 50 Bio Spectrophotometer (Agilent Technologies). In order to allow for direct comparison, TTSL and TTSL-Ab liposomes were prepared following the same steps, except for the post-insertion process where HBS (pH 7.4) was used instead of mal-PEG$_{2000}$ Ab micelles.

4.6. DOX loading and release experiments

DOX was then encapsulated into TTSL and TTSL-Ab liposomes by ammonium sulfate gradient method at 1:20 DOX:Lipids mass ratio by 5 h incubation at 39 C°. Details of DOX loading process are explained in SI text.

4.7. Surface plasmon resonance study of anti-MUC-1 TTSL-Ab liposome

Surface plasmon resonance study was used to confirm the anti-MUC-1 antibody binding capacity after conjugation to mal-DSPE-PEG$_{2000}$ and post-insertion into TTSL liposomes. For full details, please refer to (SI text).

4.8. Cellular binding and uptake studies

MDA-MB-435, MCF-7 and C33a were grown on glass cover slip in 24 tissue culture well plate (corning USA) at 40,000 cells per well over night to reach confluency. Imaging of cellular binding, and uptake was done using confocal laser scanning microscopy (CLSM) Zeiss LSM 710 (Obserkochen, Germany).

4.9. Cellular binding of anti-MUC-1 Ab

Experimental procedure for cellular binding of anti-MUC-1 Ab is described in SI text.

4.10. Cellular uptake of TTSL and TTSL-Ab liposomes

Cellular uptake studies of DOX-loaded and DiI-labeled TTSL and TTSL-Ab liposomes (150 μM lipids, 10 μM DOX) were performed independently due to the overlap in the fluorescent spectrum of DOX and DiI. First, to study the cellular uptake kinetics, DOX-loaded TTSL, TTSL-Ab-I, and TTSL-Ab-II uptake by MDA-MB-435 and C33a were studied after 1 h, 3 h, and 24 h incubation at 37 °C. At the end of incubation, time cells were washed with PBS to remove any unbound liposomes and then imaged with CLSM with and without 1 h heating at 42 °C, using 488 nm laser excitation source, 534 nm output filter, and EC Plan-Apochromat 40x/1.3 oil to detect DOX fluorescence signal.

The effect of antibody conjugation of the uptake of the liposomes itself by MDA-MB-435 cells was also studied after 1 h and 3 h incubation with DiI-labeled liposomes at 37 °C. At the end of incubation time, cells were washed with PBS to remove unbound liposomes then fixed with PFA 4% and visualized with CLSM using 514 nm laser excitation source, 585 nm output filter, and EC Plan-Apochromat 40x/1.3 oil to detect DiI fluorescence signal.

4.11. Cellular cytotoxicity study (MTT assay)

Cytotoxicity of DOX-loaded TTSL and TTSL-Ab was determined using MTT dye reduction assay. Briefly, MDA-MB-435 (MUC-1 + ve) and C33a (MUC-1 − ve) cells were plated in 96-well plates (Coster, USA) at 8×10^3 and 1×10^4 cells/well, respectively. Cells were incubated at 37 °C overnight before treatment and then treated with free DOX, TTSL, TTSL-Ab-I, and TTSL-Ab-II at 10 μM for 3 h at 37 °C in CO_2 Incubator. At the end of 3 h, treatment cells were then washed and replaced with liposome-free media. At this stage, plates were either incubated at 37 °C for 48 h or treated for 1 h at 42 °C in CO_2 incubator followed by incubated at 37 °C for 48 h to evaluate the effect of triggered drug release after uptake by the cells. Cell viability was then assessed with MTT assay. More details are explained in SI text.

4.12. Localization and cytotoxicity studies using multicellular spheroids (MCS)

Experimental details are explained in SI text.

4.13. Animals and tumor models

Five- to six-week-old female athymic nude mice (20–25 g) were purchased from Charles River Laboratories, UK. Animal procedures were performed in compliance with the UK Home Office code of practice for the housing and care of animals used in scientific procedures. Mice were acclimatized to the environment for at least 7 days before implantation of MDA-MB-435 tumor model. More details are explained in SI text.

4.14. Biodistribution studies of ^{14}C-DOX-loaded TTSL and TTSL-Ab-II

The effect of anti-MUC-1 antibody conjugation to TTSL on their pharmacokinetics and biodistribution parameters was also studied after *in vivo* administration. TTSL and TTSL-Ab-II were prepared in 25 mM (total lipid concentration) as described earlier and loaded with ^{14}C-DOX (equivalent to 0.2 μCi/dose) as a drug label. Mice ($n = 3$–4) were injected intravenously via tail vein under isoflurane anesthesia with 200 μl liposomes suspension (equivalent to 2.5 μmol of lipids/200 μl, DOX 5 mg/kg) in HBS. Blood profile, organs, and tumor accumulation were studied comparing three different heating protocols as described in Scheme 1. More details are explained in SI text.

4.15. ^{14}C-DOX quantification in blood and tissue samples

Details of ^{14}C-DOX quantification method are explained in SI text.

4.16. In vivo optical fluorescence imaging

Experimental details of IVIS imaging experiment are explained in SI text.

4.17. In vivo tumor growth delay and survival studies

The therapeutic activity of anti-MUC-1-targeted TTSL-Ab-II compared to non-targeted TTSL was evaluated after *in vivo* administration into MDA-MB-435 (MUC-1 + ve) tumor-bearing athymic nude mice. When the tumor volume reached 100 mm^3 (day 13 after implantation), mice were divided into groups (5–7 mice/group) and treated with single administration of TTSL and TTSL-Ab-II (5 mg/kg DOX) by intravenous injection applying hyperthermia protocol 3 (Scheme 1) with and without application of second heating 24 h after injection. Mice were also weighed and examined for any sign of toxicity twice a week. Tumors were measured with calliper as described above and the measurement was blinded to the experimental conditions. Mice were sacrificed by cervical dislocation when tumors reached 1000 mm^3.

4.18. Statistical analysis

Statistical analysis of the data was performed using Graph Pad Prism software. A two-tailed unpaired Student *t*-test and a one-way analysis of variance followed by the Tukey multiple comparison test were used and p values <0.05 considered significant.

Acknowledgments

This research work was funded by the European Commission FP7 Program SONODRUGS (NMP4-LA-2008-213706). The authors thank Dr. Wafa Al-Jamal for her advice with the development of MDA-MB-435 tumor model.

Appendix A. Supplementary data

Supporting data including; cellular binding of anti-MUC-1 Ab, conjugation of anti-MUC-1 Ab to Mal-DSPE-PEG_{2000} and SDS–PAGE analysis, quantification of anti-MUC-1 post-insertion efficiency, SPR studies, cellular binding and cellular uptake of DOX-loaded TTSL and TTSL-Ab-II liposomes by MDA-MB-435 and C33a cells, localization into MCS, and organ biodistribution of ^{14}C-DOX TTSL and TTSL-Ab-II. These materials are available free of charge via the Internet. Supplementary data associated with this article can be found in the online version at http://dx.doi.org/10.1016/j.jconrel.2014.10.013.

References

[1] M.S. Ewer, et al., Cardiac safety of liposomal anthracyclines, Semin. Oncol. 31 (6 Suppl 13) (2004) 161–181.
[2] R. Soloman, A.A. Gabizon, Clinical pharmacology of liposomal anthracyclines: focus on pegylated liposomal Doxorubicin, Clin. Lymphoma Myeloma 8 (2008) 21–32.
[3] A. Gabizon, et al., Improved therapeutic activity of folate-targeted liposomal doxorubicin in folate receptor-expressing tumor models, Cancer Chemother. Pharmacol. 66 (1) (2010) 43–52.
[4] T.M. Allen, Ligand-targeted therapeutics in anticancer therapy, Nat. Rev. Cancer 2 (2002) 750–763.
[5] V. Torchilin, Antibody-modified liposomes for cancer chemotherapy, Expert Opin. Drug Deliv. 5 (2008) 1003–1025.
[6] C. Mamot, D.C. Drummond, U. Greiser, K. Hong, D.B. Kirpotin, J.D. Marks, J.W. Park, Epidermal growth factor receptor (EGFR)-targeted immunoliposomes mediate specific and efficient drug delivery to EGFR- and EGFRvIII-overexpressing tumor cells, Cancer Res 63 (2003) 3154–3161.
[7] J.W. Park, et al., Tumor targeting using anti-her2 immunoliposomes, J. Control. Release 74 (2001) 95–113.
[8] D.B. Kirpotin, et al., Antibody targeting of long-circulating lipidic nanoparticles does not increase tumor localization but does increase internalization in animal models, Cancer Res. 66 (2006) 6732–6740.
[9] T. Lammers, Drug targeting to tumors: principles, pitfalls and (pre-) clinical progress, J. Control. Release 161 (2012) 175–187.
[10] D. Needham, G. Anyarambhatla, G. Kong, M.W. Dewhirst, A new temperature-sensitive liposome for use with mild hyperthermia: characterization and testing in a human tumor xenograft model, Cancer Res. 60 (2000) 1197–1201.
[11] C.D. Landon, J.Y. Park, D. Needham, M.W. Dewhirst, Nanoscale drug delivery and hyperthermia: the materials design and preclinical and clinical testing of low temperature-sensitive liposomes used in combination with mild hyperthermia in the treatment of local cancer, Open Nanomed. J. 3 (2011) 38–64.
[12] www.celsion.com2013.
[13] S.M. Sullivan, L. Huang, Enhanced delivery to target cells by heat-sensitive immunoliposomes, Proc. Natl. Acad. Sci. U. S. A. 83 (16) (1986) 6117–6121.
[14] A. Puri, et al., HER2-specific affibody-conjugated thermosensitive liposomes (affisomes) for improved delivery of anticancer agents, J. Liposome Res. 18 (2008) 293–307.
[15] B. Smith, et al., Hyperthermia-triggered intracellular delivery of anticancer agent to HER2(+) cells by HER2-specific affibody (ZHER2-GS-Cys)-conjugated thermosensitive liposomes (HER2(+) affisomes), J. Control. Release 153 (2011) 187–194.
[16] M. Kullberg, K. Mann, J.L. Owens, A two-component drug delivery system using Her-2-targeting thermosensitive liposomes, J. Drug Target. 17 (2009) 98–107.
[17] M. Kullberg, J.L. Owens, K. Mann, Listeriolysin O enhances cytoplasmic delivery by Her-2 targeting liposomes, J. Drug Target. 18 (2010) 313–320.
[18] P. Pradhan, et al., Targeted temperature sensitive magnetic liposomes for thermo-chemotherapy, J. Control. Release 142 (2010) 108–121.
[19] J.M. Limacher, B. Acres, MUC1, a therapeutic target in oncology, Bull. Cancer 94 (2007) 253–257.
[20] E.H. Moase, et al., Anti-MUC-1 immunoliposomal doxorubicin in the treatment of murine models of metastatic breast cancer, Biochim. Biophys. Acta 1510 (2001) 43–55.
[21] M.H. Gaber, et al., Thermosensitive liposomes: extravasation and release of contents in tumor microvascular networks, Int. J. Radiat. Oncol. Biol. Phys. 36 (5) (1996) 1177–1187.
[22] M. de Smet, E. Heijman, S. Langereis, N.M. Hijnen, H. Grüll, Magnetic resonance imaging of high intensity focused ultrasound mediated drug delivery from temperature-sensitive liposomes: an *in vivo* proof-of-concept study, J. Control. Release 150 (2011) 102–110.
[23] W.T. Al-Jamal, Z.S. Al-Ahmady, K. Kostarelos, Pharmacokinetics & tissue distribution of temperature-sensitive liposomal doxorubicin in tumor-bearing mice triggered with mild hyperthermia, Biomaterials 33 (2012) 4608–4617.
[24] J.N. Moreira, T. Ishida, R. Gaspar, T.M. Allen, Use of the post-insertion technique to insert peptide ligands into pre-formed stealth liposomes with retention of binding activity and cytotoxicity, Pharm. Res. 19 (2002) 265–269.
[25] S. Sofou, G. Sgouros, Antibody-targeted liposomes in cancer therapy and imaging, Expert Opin. Drug Deliv. 5 (2008) 189–204.
[26] C.-W. Chen, Novel RGD-lipid conjugate-modified liposomes for enhancing siRNA delivery in human retinal pigment epithelial cells, Int. J. Nanomedicine 6 (2011) 2567–2580.
[27] F.Y. Yang, et al., Pharmacokinetic analysis of 111 in-labeled liposomal doxorubicin in murine glioblastoma after blood-brain barrier disruption by focused ultrasound, PLoS One 7 (9) (2012) e45468.
[28] G. Kong, R.D. Braun, M.W. Dewhirst, Characterization of the effect of hyperthermia on nanoparticle extravasation from tumor vasculature, Cancer Res. 61 (2001) 3027–3032.
[29] A. Gabizon, et al., Prolonged circulation time and enhanced accumulation in malignant exudates of doxorubicin encapsulated in polyethylene-glycol coated liposomes, Cancer Res. 54 (1994) 987–992.
[30] F. Pastorino, et al., Targeting liposomal chemotherapy via both tumor cell–specific and tumor vasculature–specific ligands potentiates therapeutic efficacy, Cancer Res. 66 (2006) 10073–10082.
[31] A. Fondell, et al., *In vitro* evaluation and biodistribution of HER2-targeted liposomes loaded with an 125I-labelled DNA-intercalator, J. Drug Target. 19 (2011) 846–855.
[32] A.N. Lukyanov, T.A. Elbayoumi, A.R. Chakilam, V.P. Torchilin, Tumor-targeted liposomes: doxorubicin-loaded long-circulating liposomes modified with anti-cancer antibody, J. Control. Release 100 (2004) 135–144.
[33] D.E. Lopes de Menezes, L.M. Pilarski, T.M. Allen, *In vitro* and *in vivo* targeting of immunoliposomal doxorubicin to human B-cell lymphoma, Cancer Res. 58 (1998) 3320–3330.
[34] T.A. Elbayoumi, V.P. Torchilin, Tumor-specific anti-nucleosome antibody improves therapeutic efficacy of doxorubicin-loaded long-circulating liposomes against primary and metastatic tumor in mice, Mol. Pharm. 6 (2009) 246–254.
[35] X.B. Xiong, et al., Enhanced intracellular uptake of sterically stabilized liposomal Doxorubicin *in vitro* resulting in improved antitumor activity *in vivo*, Pharm. Res. 22 (6) (2005) 933–939.
[36] X.B. Xiong, et al., Intracellular delivery of doxorubicin with RGD-modified sterically stabilized liposomes for an improved antitumor efficacy: *in vitro* and *in vivo*, J. Pharm. Sci. 94 (2005) 1782–1793.
[37] C. Mamot, et al., Epidermal growth factor receptor-targeted immunoliposomes significantly enhance the efficacy of multiple anticancer drugs *in vivo*, Cancer Res. 65 (2005) 11631–11638.
[38] M. Juweid, et al., Microphamacology of monoclonal antibodies in solid tumors: direct experimental evidence for a binding site barrier, Cancer Res. 52 (1992) 5144–5153.
[39] P. Sapra, T.M. Allen, Internalizing antibodies are necessary for improved therapeutic efficacy of antibody-targeted liposomal drugs, Cancer Res. 62 (2002) 7190–7194.
[40] R. Suzuki, et al., Effective anti-tumor activity of oxaliplatin encapsulated in transferrin-PEG-liposome, Int. J. Pharm. 346 (2008) 143–150.
[41] F. Pastorino, et al., Vascular damage and anti-angiogenic effects of tumor vessel-targeted liposomal chemotherapy, Cancer Res. 63 (2003) 7400–7409.
[42] P. Sapra, T.M. Allen, Improved outcome when B-cell lymphoma is treated with combinations of immunoliposomal anticancer drugs targeted to both the CD19 and CD20 epitopes, Clin. Cancer Res. 10 (2004) 2530–2537.

[43] L. Eikenes, Hyaluronidase induces a transcapillary pressure gradient and improves the distribution and uptake of liposomal doxorubicin (Caelyx) in human osteosarcoma xenografts, Br. J. Cancer 93 (2005) 81–88.
[44] L. Davies, et al., Radiation improves the distribution and uptake of liposomal doxorubicin (caelyx) in human osteosarcoma xenografts, Cancer Res. 64 (2004) 547–553.
[45] G. Kong, M.W. Dewhirst, Hyperthermia and liposomes, Int. J. Hyperthermia 15 (1999) 345–370.
[46] D.A. Cope, M.W. Dewhirst, H.S. Friedman, D.D. Bigner, M.R. Zalutsky, Enhanced delivery of a monoclonal antibody F(ab')2 fragment to subcutaneous human glioma xenografts using local hyperthermia, Cancer Res. 50 (1990) 1803–1809.
[47] J.M. Schuster, et al., Hyperthermic modulation of radiolabeled antibody uptake in a human glioma xenograft and normal-tissues, Int. J. Hyperthermia 11 (1995) 59–72.
[48] M.L. Hauck, M.W. Dewhirst, D.D. Bigner, M.R. Zalutsky, Local hyperthermia improves uptake of a chimeric monoclonal antibody in a subcutaneous xenograft model, Clin. Cancer Res. 3 (1997) 63–70.
[49] G. Kong, R.D. Braun, M.W. Dewhirst, Hyperthermia enables tumor-specific nanoparticle delivery: effect of particle size, Cancer Res. 60 (2000) 4440–4445.
[50] T. Karino, S. Koga, M. Maeta, Experimental studies of the effects of local hyperthermia on blood flow, oxygen pressure and pH in tumors, Jpn. J. Surg. 18 (1988) 276–283.
[51] K. Fujiwara, T. Watanabe, Effects of hyperthermia, radiotherapy and thermoradiotherapy on tumor microvascular permeability, Acta Pathol. Jpn. 40 (1990) 79–84.
[52] A.H. Negussie, et al., Synthesis and *in vitro* evaluation of cyclic NGR peptide targeted thermally sensitive liposome, J. Control. Release 143 (2010) 265–273.
[53] A. Bandekar, et al., Antitumor efficacy following the intracellular and interstitial release of liposomal doxorubicin, Biomaterials 33 (2012) 4345–4352.
[54] D.L. Iden, T.M. Allen, *In vitro* and *in vivo* comparison of immunoliposomes made by conventional coupling techniques with those made by a new post-insertion approach, Biochim. Biophys. Acta 1513 (2001) 207–216.
[55] T. Yang, et al., Preparation and evaluation of paclitaxel-loaded PEGylated immunoliposome, J. Control. Release 120 (2007) 169–177.